High-Security 3D-CAP Modulation Based on Triple-Decker Constellation in a 7-Core Fiber

Siqi He, Bo Liu, Jianxin Ren, Rahat Ullah, Xiangyu Wu, Yaya Mao, Shuaidong Chen, Chenqi Ni, Tutao Wang, Yiming Ma, Chenfang Zhang, He Zhang, Shikui Shen, and Guangquan Wang

***Abstract*—In this paper, a high-security three-dimensional carrier-less amplitude-phase (3D-CAP) modulation is proposed, which can be used for short-distance multi-core fiber communication. Using a brand-new 3D constellation dubbed Triple-Decker, the 3D-CAP passive optical network's bit error rate (BER) performance is improved. This constellation's constellation figure of merit can be increased by changing the three-dimensional constellation distribution through geometric shaping. To provide constellation encryption for Triple-Decker by rotation, expansion, and time slot scrambling at the physical layer in 3D-CAP passive optical network (3D-CAP-PON), a four-dimensional hyperchaotic system known as Fu's model is utilized. We successfully carried out an experiment demonstrating 25.5 Gb/s 3D-CAP transmission over a 7-core fiber communication system. Experimental results illustrate that, compared to the traditional 3D constellation, our suggested scheme can obtain 0.6 dB receiving sensitivity gain at the BER$\sim$1 $\times$ 10^{-3}. The achieved key space is 10^{120}. Due to its strong security and superior performance, this scheme has a promising future in short-distance secure communication.**

***Index Terms*—High-security, three-dimensional carrier-less amplitude-phase, 7-core fiber.**

I. Introduction

With the rapid development of new-generation broadband multimedia services such as 5G, virtual reality applications, and mobile edge computing, the demands for high-speed internet and high-capacity networks are growing exponentially [1]. Due to the benefits, including fast transmission rate, colossal bandwidth, low cost, and the capacity to deliver multiple services, the passive optical network (PON) technology has been rapidly adopted worldwide [2], [3], [4]. The intensity modulation and direct detection (IM/DD) system has become the most practical and technical solution for short and medium-distance transmission systems because of its attractive features such as low cost, low power consumption, and simple structure. One of the advanced IM/DD-based modulation formats named carrier-less amplitude phase (CAP) modulation is a low-cost modulation format to increase the data transmission rate [5], [6], [7]. CAP substitute mutually orthogonal shaping filters for carrier multiplication to form quadrature signals in the modulation process. The CAP has been expanded to three-dimensional, four-dimensional, and even higher dimensions to increase the communication system's adaptability for various sorts of subscribers [8].

Furthermore, we may get a more tremendous minimal Euclidean distance (MED) in high-dimensional constellations while using the same amount of energy. While to effectively improve spectral efficiency, geometric shaping (GS) has attracted much attention as a typical modulation format optimization technique. The basic principle of GS is to optimize the geometric distribution design of constellation points by considering factors such as the MED, channel noise, and symmetry to decrease the gap between the initial constellation and Shannon capacity. A unique constellation-based star-shaped CAP-16/32 modulation that can boost the bit error rate (BER) performance and the constellation figure of merit (CFM) was presented in [9].

Space division multiplexing (SDM) has been suggested as a new efficient way to solve the capacity crisis because the standard single-mode fiber is already getting close to the physical limit established by the Shannon. This is due to the growing high capacity interconnection demand by the end-users [10], [11], [12]. SDM mainly includes core multiplexing based on multi-core fiber (MCF) and mode multiplexing based on few-mode fiber (FMF). The crosstalk between different modes of FMF is serious, and a complex equalization algorithm is required to recover the signal at the receiving end. While MCF contains multiple parallel cores in the same cladding, where each core can be utilized as an independent transmission channel for signal, what's more, the crosstalk between cores is minimal, and the fiber structure is more straightforward.

Manuscript received 2 August 2022; revised 23 August 2022; accepted 25 August 2022. Date of publication 29 August 2022; date of current version 12 September 2022. The work was supported in part by the National Key Research and Development Program of China under Grant 2018YFB1800901, in part by the National Natural Science Foundation of China under Grants 61835005, 62171227, 61727817, U2001601, 62035018, 61875248, 61935005, 61935011, 61720106015, and 61975084, in part by the Natural Science Foundation of the Jiangsu Higher Education Institutions of China under Grant 22KJB510031, in part by the Jiangsu team of Innovation and Entrepreneurship, and in part by The Startup Foundation for Introducing Talent of NUIST, Postgraduate Research & Practice Innovation Program of Jiangsu Province under Grant SJCX22_0346. *(Corresponding author: Bo Liu).*

Siqi He, Bo Liu, Jianxin Ren, Rahat Ullah, Xiangyu Wu, Yaya Mao, Shuaidong Chen, Chenqi Ni, Tutao Wang, and Yiming Ma are with the Institute of Optics and Electronics, Nanjing University of Information Science and Technology, Nanjing 210044, China, with the Jiangsu Key Laboratory for Optoelectronic Detection of Atmosphere and Ocean, Nanjing University of Information Science & Technology, Nanjing 210044, China, and also with the Jiangsu International Joint Laboratory on Meteorological Photonics and Optoelectronic Detection, Nanjing University of Information Science & Technology, Nanjing 210044, China (e-mail: siqi7kiki@163.com; bo@nuist.edu.cn; 003458@nuist.edu.cn; rahat@nuist.edu.cn; wxyhairuo@sina.com; 002807@nuist.edu.cn; 1678612644@qq.com; 1686961728@qq.com; 1920765116@qq.com; 792036122@qq.com).

Chenfang Zhang, He Zhang, Shikui Shen, and Guangquan Wang are with China Unicom Research Institute, Beijing 100048, China (e-mail: zhangcf80@chinaunicom.cn; zhanghe35@chinaunicom.cn; shensk@chinaunicom.cn; wanggq122@chinaunicom.cn).

Digital Object Identifier 10.1109/JPHOT.2022.3202657

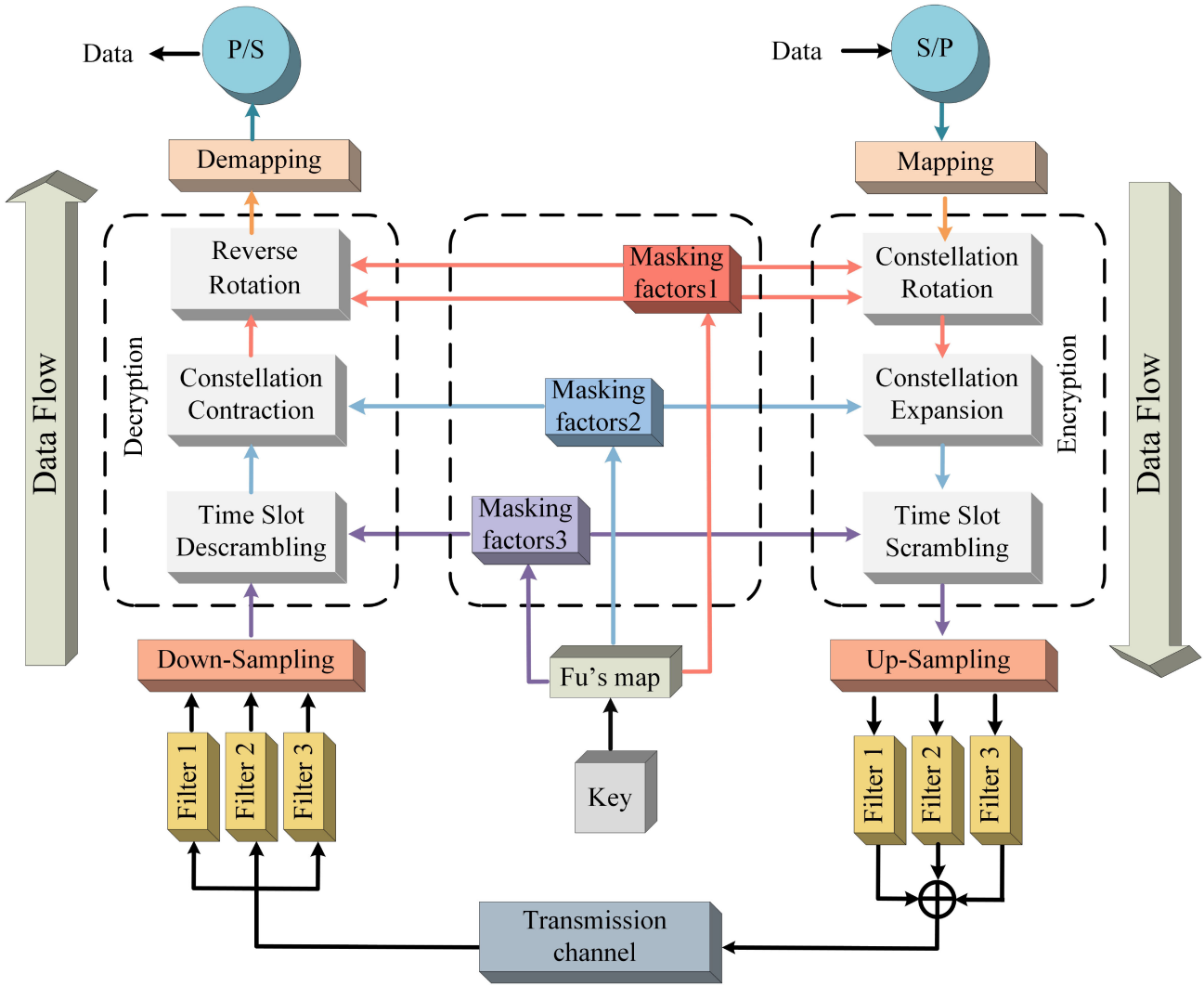

Fig. 1. The schematic diagram of high security 3D-CAP modulation based on Triple-Decker.

To maintain information security in the broadcast mechanism of the PON design, channel transmission capacity must be increased. Through machine learning, the conventional transmission layer or protocol stack layer encryption technique can be recognized and decoded. Numerous studies have revealed that the encryption, which is based on the offline digital signal processing (DSP) method in the physical layer and is directed to the optical fiber transmission channel, can successfully guarantee the security of the communication transmission. Chaos is an unpredictable, random-like form of motion. The chaotic data encryption has inherent randomness, initial value sensitivity, and irregular order and does not require the support of complex hardware systems [13], [14]. It is an effective means to enhance the safety performance of communication systems and can more effectively ensure the information's security. To achieve high security through effective encryption, the development of a secure optical three-dimensional probabilistically shaped CAP system based on spherical constellation masking is reported in [15]. In [16], the authors presented a two-stage spherical constellation masking-based security-enhanced three-dimensional CAP passive optical network (3D-CAP-PON). Numerous studies have demonstrated how the security of the spherical constellation masking approach, which encrypts signals using chaotic sequences, is fairly guaranteed. Compared with chaotic systems, hyperchaotic systems have two or more positive Lyapunov indices and more complex dynamic characteristics, which have higher practical value in the field of information security.

In this study, we suggested a high-security 3D-CAP modulation based on a Triple-Decker constellation in a 7-core Fiber with greater CFM, which successfully decreased the BER and enhanced the signal quality. Then, we used Fu's model, a four-dimensional hyperchaotic system, to create hyperchaotic sequences for the unique constellation diagram's encryption. In 3D-CAP-PON, three stages of constellation masking—rotation, expansion, and time scrambling are utilized. To achieve the goal of information encryption and boost the overall security of the optical network, the signal in the transmission channel behaves like random noise. We successfully implemented the

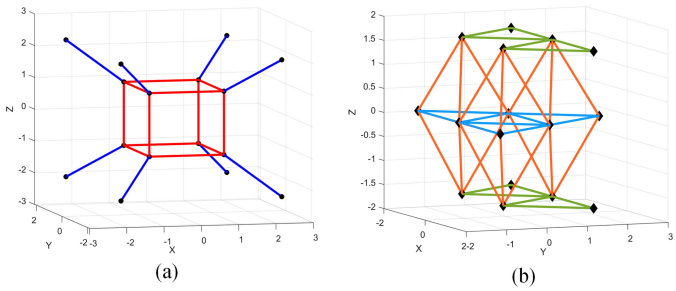

Fig. 2. (a) the traditional constellation; (b) a new design of 16-ary 3D constellation named Triple-Decker.

transmission of our innovative technique over a 2 km 7-core optical fiber to demonstrate its practicality.

II. Principles

A. Principles of Triple-Decker Constellation

The schematic diagram of high-security 3D-CAP modulation based on Triple-Decker is depicted in Fig. 1. At the transmitting end, the binary data is converted into three parallel signal streams after serial-parallel (S/P) conversion, and three-dimensional constellation mapping is performed to form a new three-dimensional constellation point distribution. We have generated a total of 25000 3D constellation points, among which 1000 constellation points are used as training sequences for channel estimation, and the rest are utilized for information transmission. After that, the hyperchaotic sequences generated by Fu's model are used to mask the constellation points and achieve three-level encryption. The original constellation distribution is transformed into a disorder sphere, and then the three mutually orthogonal shaping filters are used to realize the shaping and filtering of the three-way signal. After shaping and filtering, the 3D-CAP signal can be transmitted into different fiber transmission channels, such as multi-core fibers, single-mode fibers, few-mode fibers and so on. In order to verify the feasibility of our scheme, we successfully realized the transmission of the scheme over a 2 km 7-core optical fiber. The matched filter bank corresponding to the shaping filter is used at the receiving end to divide the obtained signal into three channels for processing. The demodulation and decryption of the signal can be realized by the inverse process.

The 16-ary 3D constellations of two different geometries is shown in Fig. 2, where Fig. 2(a) is the traditional and the straightforward distribution of 16-ary constellation points, and its 16 constellation points are distributed on the eight vertices of the inner and outer cubes respectively. Fig. 2(b) is a new design of a layered symmetric 16-ary 3D constellation named Triple-Decker. Since the equilateral triangle in the two-dimensional space is the regular polygon with the nearest distance between the vertex and the center, the 2D constellation diagram usually takes the standard triangle as the basic unit, which can effectively concentrate on the constellation points around the origin. For the same reason, we often use regular tetrahedrons as the basic unit in three-dimensional space. In the 3D constellation design of Triple-Decker, regular tetrahedrons and regular triangles are used to complete the distribution of 16 constellation points. The specific method distributes these constellation points on three two-dimensional planes with different z-axis values. The two-dimensional plane with a z-axis value of 0 is the middle plane. The horizontal and vertical coordinates of the upper and lower constellation points are the same, where the z-axis coordinate values are opposite to each other. The exact constellation point coordinates and mapping rules are given in Table I, and in this paper, the MED $d_{\min}$ is 2.

The performance of the constellation diagram is closely related to MED and average energy. Under the condition of an equal signal-to-noise ratio (SNR), better noise immunity will be achieved for a larger MED. The constellation's sensitivity to noise decreases with decreasing average power when the MED is fixed. So the bit error performance of the constellation is expected to be better. But the average energy will change with the change of MED. If we blindly increase the MED in order to seek better system performance, the average energy will also increase, which will affect the bit error performance of the constellation diagram. Therefore, we describe the efficiency of the constellation by the ratio of $d_{\min}^2$to the average power of the constellation, which can be defined as the CFM [17]:

$$CFM = \frac{d_{min}^2}{P} \tag{1}$$

According to equation (1), the CFM of the traditional constellation is 0.4726, while the CFM of Fig. 2(b) is 0.8421. It can be seen that this new type of 3D constellation pattern has obtained a significant improvement.

B. Encryption Based on Triple-Decker Constellation

In addition, we use a four-dimensional hyperchaotic system as the chaotic mapping model and generate masking vectors to encrypt the constellation. The dynamic equation of the four-dimensional hyperchaotic system is:

$$\begin{cases} \frac{dx}{dt} = -ax + yz \\ \frac{dy}{dt} = xz - y^3 \\ \frac{dz}{dt} = -bxy + cz + \omega \\ \frac{d\omega}{dt} = y - dz \end{cases} \tag{2}$$

In the above equation (2), When the control parameters of the system $[a, b, c, d] = [6, 4, 8, 2]$, the four state variable initial values $[x_0, y_0, z_0, \omega_0] = [1, 2, 3, 4]$, it means the system is in a hyperchaotic state, and the phase portrait of the hyperchaotic attractors is demonstrated in Fig. 3.

We convert the constellation points represented by the three-dimensional Cartesian coordinate system into the spherical coordinate system, $P(x, y, z)$ corresponding to $P(r, \theta, \varphi)$, where $r = \sqrt{x^2 + y^2 + z^2}$; $\theta$is the angle between the directional line segment OP and the positive z-axis, called the elevation angle; $\varphi$is called the azimuth angle, which is the angle between the projection line of the line from the origin to the point P on the x-y plane and the x-axis.

TABLE I
PARAMETERS OF THE TRADITIONAL CONSTELLATION AND TRIPLE-DECKER

number	the traditional spatial coordinates	mapping rules	Triple-Decker's spatial coordinates
1	(1,-1,-1)	1101	(-1,0.5774,0)
2	(1,1,-1)	1100	(1,0.5774,0)
3	(-1,1,-1)	1000	(0,-1.1547,0)
4	(-1,-1,-1)	1001	(-2,-1.1547,0)
5	(1,-1,1)	1111	(0,2.3094,0)
6	(1,1,1)	1010	(2,-1.1547,0)
7	(-1,1,1)	1110	(-1,-0.5774,1.6330)
8	(-1,-1,1)	1011	(0,1.1547,1.6330)
9	(2.1547,-2.1547,-2.1547)	0101	(1,-0.5774,1.6330)
10	(2.1547, 2.1547,-2.1547)	0100	(-1,-0.5774,-1.6330)
11	(-2.1547, 2.1547,-2.1547)	0000	(0,1.1547,-1.6330)
12	(-2.1547,- 2.1547,- 2.1547)	0001	(1,-0.5774,-1.6330)
13	(2.1547,- 2.1547, 2.1547)	0111	(-2,1.1547,1.6330)
14	(2.1547,2.1547, 2.1547)	0110	(2,1.1547,1.6330)
15	(-2.1547, 2.1547, 2.1547)	0010	(-2,1.1547,-1.6330)
16	(-2.1547, -2.1547, 2.1547)	0011	(2,1.1547,-1.6330)

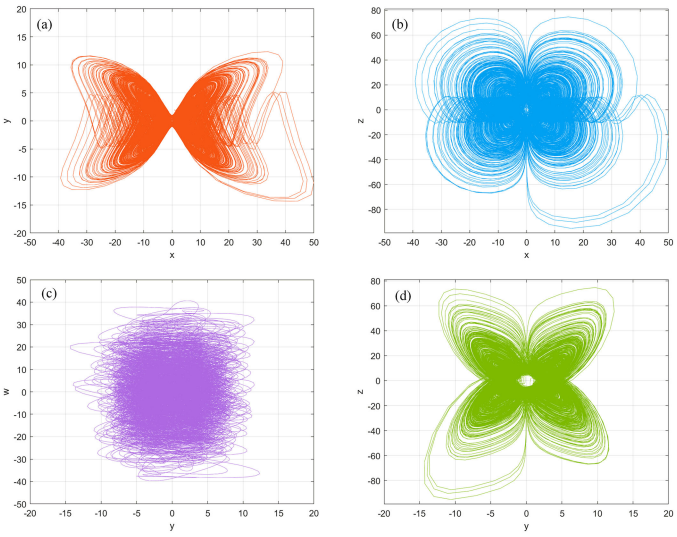

Fig. 3. Phase portrait of Fu's model.

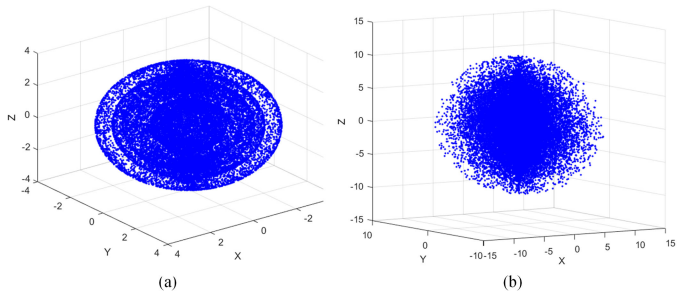

Fig. 4. Constellation diagrams (a) After rotation masking; (b) After expansion masking.

For the hyperchaotic sequences $[x_1, y_1, z_1, \omega_1]$ generated by the Fu's model, we use x_1 and y_1 to generate the masking vectors for constellation rotation, and the rotation angle rules are set as:

$$\begin{cases} \rho_1 = mod\left(x_1 \times 10^{10}, \pi\right), \rho_1 \in (0, \pi) \\ \rho_2 = mod\left(y_1 \times 10^{10}, 2\pi\right) - \pi, \rho_2 \in (-\pi, \pi) \end{cases} \tag{3}$$

The change of elevation angle is $\theta' = \theta + \rho_1$, therefore, the elevation angle of the original constellation point that can be rotated in the range of $(0, \pi)$. Similarly, the complete coverage rotation encryption within the range of $(-\pi, \pi)$ is possible when the azimuth angle changes according to the $\varphi' = \varphi + \rho_2$ formula. After two angular rotation encryptions, the first-level encrypted constellation point distribution based on constellation rotation masking can be obtained, as shown in Fig. 4(a). At this time, the constellation points are transformed into four hollow spheres with different radii.

Next, we used z_1 to generate the masking factor of constellation expansion for second-level encryption; the rule can be given as:

$$r_1 = floor\left(mod\left(z_1 \times 10^{10}, 50\right)\right)/50 \times 2 + 1, r_1 \in [1, 3] \tag{4}$$

The changing relationship of the radius is $r' = r * r_1$, after the expansion of the radius, the original four-layer hollow sphere can be disturbed into a solid sphere as shown in Fig. 4(b).

After that, to further improve the security of the transmission process, we use the masking factor ω_1 to generate a time slot scrambling for the third-level encryption. The specific rule is

$$\omega_2 = floor\left(mod\left(\omega_1 \times 10^{10}, 100\right)\right) + 1, \omega_2 \in [1, 100] \tag{5}$$

In the newly generated ω_2 sequence, randomly select three numbers to scramble and transform r', θ', φ'. For example, we randomly select the 36th, 58th, and 79th bits of data, which are 6, 47, and 20, respectively. Fig. 5 demonstrates the scrambling rule. After this, the r', θ', φ' encrypted by the rotation and scaling are completely disrupted again, and the scrambling degree reaches

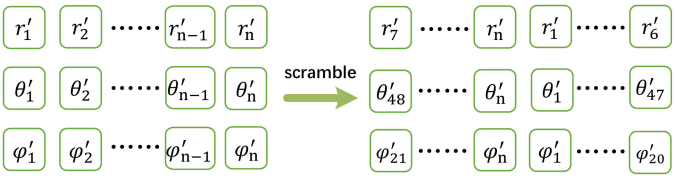

Fig. 5 The schematic diagram of the scrambling rule.

100%. In the process of the time slot scrambling, we only change the transmission sequence of the signal, but not the amplitude. This scheme has little impact on peak to average power ratio of the signal.

We add a frame header in front of the CAP signal for synchronization. Without the proper key information, unauthorized optical network units (ONUs) can only steal dense, spherical constellation diagrams that resemble noise after three levels of constellation perturbation encryption through rotation, expansion, and scrambling.

III. Experimental Setup and Results

A. Experimental Setup

We performed the experimental procedure depicted in Fig. 6 in order to confirm how well spherical encryption performed on the brand-new Triple-Decker constellation. The experiment uses a light source with a 1550 nm wavelength and a 12 dBm power level. The entire system uses the following transmission mechanism.

The encrypted signal generated by offline Tx-DSP of the original data is imported into an arbitrary waveform generator (AWG) for digital-to-analog conversion (DAC) of the encrypted signal at 10 GSa/s. The signal is amplified by an electric amplifier (EA) and then projected into a Mach-Zehnder modulator (MZM) to produce a modulated optical signal, which can be amplified through an Erbium-doped fiber amplifier (EDFA) to compensate for the power losses. Then, a power splitter (PS) is used to divide the signal into 8 parts, and the correlation between the signal is removed through the delay line. Each independent part is fanned into a 2 km weakly coupled 7-core fiber for transmission. The employed 7-core fiber is a commercially procured weakly coupled multi-core fiber with single core diameter of 8 μm and core pitch of 41.5 μm. The coating diameter is 245 μm, which is limited to 250 μm in order to maintain the mechanical reliability [18]. In addition, the average core insertion loss is about 1.5 dB, and the crosstalk between the adjacent cores is less than -50 dB [19]. The optical signal is then demultiplexed into 7 single-mode fibers by fanning out. Through a PS, the optical signal in the single-mode fiber can be distributed to various ONUs. We use a variable optical attenuator (VOA) at the ONU to modify the input optical power. The optical signal is then translated into an electrical signal by a photodetector (PD) with a bandwidth of 40 GHz. The electrical signal is then gathered using a mixed-signal oscilloscope (MSO), with a sampling rate of 50 GSa/s. The analog-to-digital conversion (ADC) is completed in the interim. Notably, given the proper key, offline Rx-DSP allows us to recover the original data.

B. Experimental Results and Analysis

Fig. 7 plots the BER curves of Triple-Decker in 7-core fiber after 2 km transmission. It is worth mentioning that with the increasing received optical power, the BER curve presents a downward trend, and there is little difference between the seven BER curves. When BER is 1×10^{-3}, the received optical power of core 1 to 7 is -20.2 dBm, -20.1 dBm, -20.1 dBm, -19.9 dBm, -18.8 dBm, -19.0 dBm and -19.5 dBm, respectively. The gap between the best core 1 and the worst core 5 is 1.4 dB, which proves that each core of the 7-core fiber in this experiment has certain homogeneity and stability.

In addition, BER curves of the traditional constellation and Triple-Decker in core 1 are shown in Fig. 8. Although the BER of the traditional constellation is lower when the optical power is low when the optical power is between -23 dBm and -18 dBm, the BER of Triple-Decker is improved compared with the traditional constellation. The results also show that the B2B transmission performance is close to that of 2 km 7-core fiber. This is because the 7-core fiber used in our experiment has high isolation degree between cores and small crosstalk. Besides, the transmission length is 2 km which has little impact on signal damage. The BER performance of the conventional constellation and Triple-Decker deteriorates and has nonlinear change at low received optical power due to the severe noise interference. This leads to a significant offset of constellation points in reception, so the system's BER performance deteriorates. Because the constellation points of the traditional one are scattered, the probability of error in judgment will be less than Triple-Decker. Overall, the advantages of Triple-Decker are apparent. When the BER is 1×10^{-3}, the optical power gain of Triple-Decker is 0.6 dB higher than that of the traditional constellation, which indicates that the new 3D constellation has obvious advantages. Constellation diagrams of the conventional constellation and Triple-Decker at -20 dBm at the receiver are also attached.

Fig. 9 shows the BER curves of the legal ONU1 and the illegal receiver after transmission through core 1 in the 7-core fiber. When the received optical power is -16 dBm, obviously that there is a difference between the three-dimensional constellation graphs of the ONU1 and the illegal receiver. In the experiment, the parameters of Fu's model are known to the legal ONU because of having the correct keys, which are unknown to the illegal ONU. As can be seen from the Fig. 9, with the increase of the received optical power, the BER of the legal ONU shows a trend of gradual decline, and a relatively clear constellation diagram can be obtained. The unauthorized ONU without a key, on the other hand, stays at a BER of about 0.5, producing a crowded, dense sphere of constellations. The proposed encryption strategy can guarantee system security and prevent illegal receivers from obtaining any reliable data unless it has the right key information.

We test the hyperchaotic model's sensitivity to the starting value to investigate the security of the data encryption in this method. Fig. 10 displays the -16 dBm receiving optical power curves after the initial value varies somewhat following

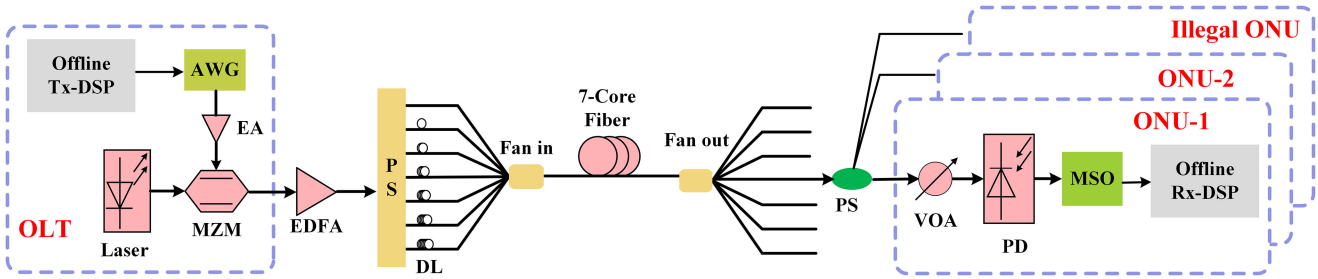

Fig. 6 Experimental setup (AWG, arbitrary waveform generator; EA, electrical amplifier; MZM, Mach-Zehnder modulator; EDFA, Erbium-doped fiber amplifier; PS, power splitter; VOA, variable optical attenuator; PD: Photodiode; MSO: Mixed-signal oscilloscope).

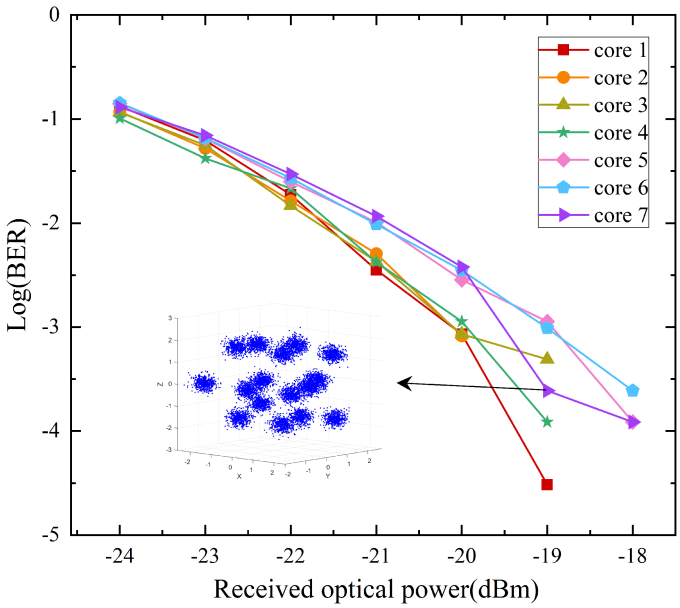

Fig. 7. BER curves of Triple-Decker in 7-core fiber after 2 km transmission.

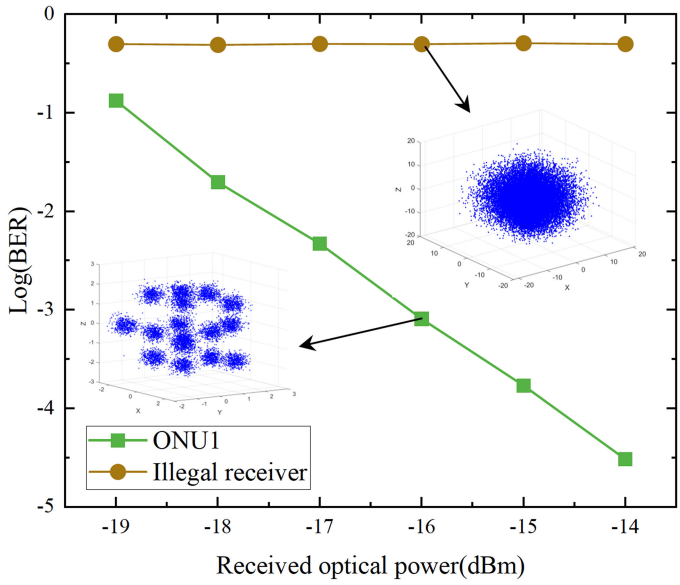

Fig. 9. BER curves of ONU1 and illegal receiver.

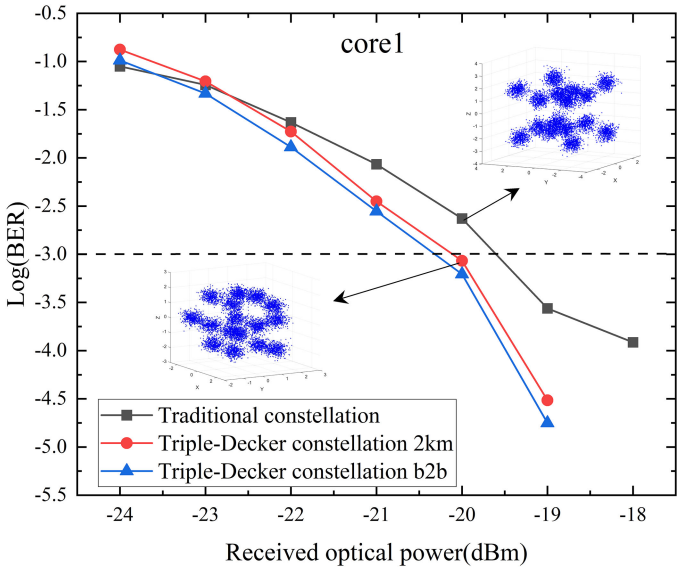

Fig. 8. BER curves of the traditional constellation and Triple-Decker in core 1.

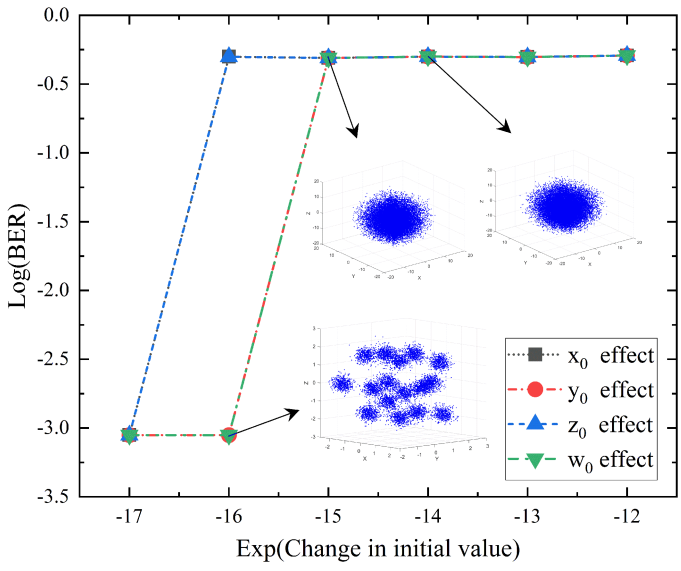

Fig. 10. BER measurements with a tiny change in the initial value.

transmission through core 1. The initial values $(x_0, y_0, z_0, \omega_0)$ of Fu's model are set to$(1, 2, 3, 4)$. For these four initial values, we can see from Fig. 10 that when the initial value of x_0 changes to 10^{-17}, BER is close to the correct parameter value. When the initial value is changed by 10^{-16}, BER will increase sharply. After the initial value increases further, BER will remain unchanged at about 0.49. The same thing happens to z_0. For the other two initial values, the system's BER remains stable when the initial values vary by 10^{-15} or more. Therefore, for our hyperchaotic model, there are altogether 8 parameters, and at least the key space that can be obtained is $(10^{15})^8 = 10^{120}$, which can delay the time for the illegal ONU to find the correct key and effectively resist the attack of stealing the right key.

IV. Conclusion

In this manuscript, we proposed a high-security 3D-CAP modulation based on the Triple-Decker constellation in a 7-core Fiber. First, we designed a new 3D constellation named Triple-Decker, whose CFM can reach 0.8421, 0.3695 higher than the traditional constellation. At the same time, Fu's model is adopted to generate hyperchaotic sequences to achieve three-dimensional constellation encryption through rotation, expansion, and time slot scrambling at the physical layer in 3D-CAP-PON. The experiment of 7-core fiber transmission shows that the average optical power gain of Triple-Decker is 0.6 dB higher than that of the traditional constellation when the BER is$\sim 1 \times 10^{-3}$. Conservatively, the proposed encryption scheme has a key space of 10^{120}. Here, the superiority of the suggested technique in MCF transmission to boost communication capacity is successfully proved; hence it has a promising future.

References

[1] V. Houtsma, D. van Veen, and E. Harstead, "Recent progress on standardization of next-generation 25, 50, and 100G EPON," *J. Lightw. Technol.*, vol. 35, no. 6, pp. 1228–1234, Mar. 2017.

[2] E. Harstead, D. Van Veen, V. Houtsma, and P. Dom, "Technology roadmap for time-division multiplexed passive optical networks (TDM PONs)," *J. Lightw. Technol.*, vol. 37, no. 2, pp. 657–664, Jan. 2019.

[3] Y. Lu et al., "Orthogonal modulation application to achieve flexible migration and colorless ONUs for next generation PON," *Opt. Commun.*, vol. 403, pp. 252–256, 2017.

[4] Y. Lu, Q. Zhou, Y. Wei, M. Hu, X. Zhou, and Q. Li, "A smooth evolution to next generation PON based on orthogonal modulation," *Opt. Commun.*, vol. 339, pp. 182–184, 2015.

[5] F.-M. Wu, C.-T. Lin, C.-C. Wei, C.-W. Chen, H.-T. Huang, and C.-H. Ho, "1.1-Gb/s white-LED-based visible light communication employing carrier-less amplitude and phase modulation," *IEEE Photon. Technol. Lett.*, vol. 24, no. 19, pp. 1730–1732, Oct. 2012.

[6] A. Sheetal and H. Singh, "5×10 Gbps WDM-CAP-PON based on frequency comb using OFDM with blue LD," *Opt. Quantum Electron.*, vol. 50, no. 12, pp. 1–14, 2018.

[7] J. Liu, J. Liu, J. Lu, M. Luo, and X. Zeng, "CART-based transmission equalization for 50 Gbit/s PAM4 over 25 km SSMFin10G-class IM/DD PON," *Opt. Fiber Technol.*, vol. 55, 2020, Art. no. 102137.

[8] L. Sun, J. Du, and Z. He, "Multiband three-dimensional carrierless amplitude phase modulation for short reach optical communications," *J. Lightw. Technol.*, vol. 34, no. 13, pp. 3103–3109, Jul. 2016.

[9] J. Ren et al., "A probabilistically shaped star-CAP-16/32 modulation based on constellation design with honeycomb-like decision regions," *Opt. Exp.*, vol. 27, no. 3, pp. 2732–2746, 2019.

[10] T. Mizuno and Y. Miyamoto, "High-capacity dense space division multiplexing transmission," *Opt. Fiber Technol.*, vol. 35, pp. 108–117, Feb. 2017.

[11] P. J. Winzer, "Optical networking beyond WDM," *IEEE Photon. J.,* vol. 4, no. 2, Apr. 2012.

[12] V. J. F. Rancano et al., "Demonstration of space-to-wavelength conversion in SDM networks," *IEEE Photon. Technol. Lett.*, vol. 27, no. 8, pp. 828–831, Apr. 2015.

[13] A. Alghafis, N. Munir, M. Khan, and I. Hussain, "An encryption scheme based on discrete quantum map and continuous chaotic system," *Int. J. Theor. Phys.*, vol. 59, no. 4, pp. 1227–1240, 2020.

[14] J. Zheng and L. Liu, "Novel image encryption by combining dynamic DNA sequence encryption and the improved 2D logistic sine map," *IET Image Process.,* vol. 14, no. 11, pp. 2310–2320, Sep. 2020.

[15] S. Chen et al., "Secure optical 3D probabilistic shaping CAP system based on spherical constellation masking," *IEEE Photon. Technol. Lett.*, vol. 32, no. 18, pp. 1171–1174, Sep. 2020.

[16] J. Ren et al., "Security-enhanced 3D-CAP-PON based on two-stage spherical constellation masking," *IEEE Access*, vol. 8, pp. 111966–111973, 2020.

[17] G. D. Forney and L.-F. Wei, "Multidimensional constellations—Part I: Introduction, figures of merit, and generalized cross constellations," *IEEE J. Sel. Areas Commun.*, vol. 7, no. 6, pp. 877–892, Aug. 1989.

[18] T. Sakamoto et al., "Low-loss and low-DMD 6-mode 19-core fiber with cladding diameter of less than 250 μm," *J. Lightw. Technol.*, vol. 35, no. 3, pp. 443–449, Feb. 2017.

[19] J. Zhang et al., "Enhanced 3D-CAP modulation with information-inserted time slots for seven-core fiber transmissions," *Opt. Exp.*, vol. 28, no. 17, pp. 24991–24999, 2020.